



HHS Public Access

Author manuscript

Ophthalmic Surg Lasers Imaging Retina. Author manuscript; available in PMC 2019 August 15.

Published in final edited form as:

Ophthalmic Surg Lasers Imaging Retina. 2018 December 01; 49(12): 946–954. doi:
10.3928/23258160-20181203-07.

Structural Integrity of Individual Cone Photoreceptors after Short-Wavelength Subthreshold Micropulse Laser Therapy for Diabetic Macular Edema

Elaine M. Wells-Gray, PhD*, Nathan Doble, PhD*,†, Matthew P. Ohr, MD†, Stacey S. Choi, PhD*,†

*The Ohio State University, College of Optometry, 338 W 10th Ave, Columbus, OH, USA 43210.

†The Ohio State University, Department of Ophthalmology and Visual Science, Havener Eye Institute, 915 Olentangy River Road, Columbus, OH, USA 43212.

Abstract

Background and Objective: Subthreshold micropulse laser (SML) treatment at 577 nm has been proposed as a safe and efficacious therapy for diabetic macular edema (DME). The study objective was to evaluate the integrity of individual cone photoreceptors after SML treatment using high resolution retinal imaging.

Methods: An observational cohort study of four DME subjects treated using SML were followed over time. Cone inner and outer segment lengths (ISL/OSL) and total retinal thicknesses (TRT) were measured as the edema resolved. The primary outcome was the detection of any laser induced photoreceptor damage/change following the SML treatment using adaptive optics (AO) imaging.

Results: Individual cones observed pre-treatment remained visible, while cones that were initially obscured by the DME became more discernable after the treatment. TRT showed statistically significant thinning in half of the subjects. One subject showed no significant change while one showed a statistically significant increase in TRT despite the treatment. No subject was found to have photoreceptor damage following treatment.

Conclusions: SML at 577 nm did not result in measureable structural damage to the underlying photoreceptor layer supporting previous work that SML is a safe alternative for treating DME.

Keywords

adaptive optics; optical coherence tomography; scanning laser ophthalmoscopy; photoreceptors; cones; laser therapy; subthreshold micropulse laser; diabetic macular edema

Corresponding Author: Nathan Doble, PhD, The Ohio State University, College of Optometry, 338 W 10th Ave, Columbus, OH, USA 43210. doble.2@osu.edu, Telephone: 614-688-2052.

The authors have no relevant financial interests and no potential conflicts of interest to disclose.

Presented as a poster at The Association for Research in Vision and Ophthalmology (ARVO) Annual Conference, Baltimore, May 2017.

INTRODUCTION

Diabetes Mellitus (DM) affects 29.1 million children and adults (9.3% of the population) in the USA. Worldwide, the projected number of people with diabetes is expected to reach 552 million (1 adult in 10) by 2030.¹ One ocular manifestation of DM is diabetic macular edema (DME) which is an accumulation of fluid in the central retina that causes vision loss. The prevalence of DME among diabetics in the USA approaches 30% in adults who have had DM for 20 years or more.² Untreated, 20–30% of patients will experience a 2 fold decrease in vision within 3 years.

The Early Treatment Diabetic Retinopathy Study (ETDRS) demonstrated a significant treatment benefit of laser photocoagulation for clinically significant DME, reducing the incidence of visual loss by ~50% at 3-years.^{3,4} Despite this improvement, the treatment was not without its drawbacks. Adverse events such as central scotoma, loss of central vision, and decreased color vision have been reported, primarily as a consequence of the progressive enlargement of the laser scars from the visible burn endpoint of conventional threshold laser photocoagulation.^{5–7}

Subthreshold micropulse laser (SML) is a recent advancement in laser technology that has been found to be clinically effective without causing any laser-induced retinal injury detectable by current clinical imaging systems. SML uses low intensity micropulsed laser spots that are selectively absorbed by the RPE cells which, in turn, normalize their function by altering cytokine expression.⁸ The restructuring and stimulation of the RPE cells are thought to be responsible for a decrease in fluid from the inner retina leading to a resolution of DME.

Previous studies have shown the 810 nm wavelength SML treatment to be as effective as ETDRS laser photocoagulation⁴ due to its selective absorption by the RPE, minimal scattering, negligible absorption by media opacities and lack of absorption by intraretinal hemorrhages, retinal vessels, foveal luteal pigment or thickened neurosensory retina.^{9,10} Although studies have shown comparative effectiveness between 810-nm and 577-nm SML treatments¹¹, the efficacy of 577-nm SML treatment has been studied less extensively than the 810-nm therapy. The goal of this study was to investigate the integrity of individual cone photoreceptors after the administration of 577-nm wavelength SML treatment using an adaptive optics (AO)-optical coherence tomography (OCT)-scanning laser ophthalmoscope (SLO).

METHODS

Subjects

Four subjects (P1:P4) diagnosed with clinically significant DME were recruited from the Havener Eye Institute, Department of Ophthalmology and Visual Science at the Ohio State University (OSU). The subjects selected for this study were chosen based on the ETDRS definition of clinically significant DME as evidenced by a zone of thickening larger than one disc diameter within a disc diameter of the foveal center. They had no evidence of central involving edema through clinical OCT making them good candidates for SML treatment

rather than intravitreal anti-VEGF injection. Clinical spectral-domain (SD) OCT (Cirrus, Zeiss, Dublin, CA) was used to image the macula using the macular cube 512 × 128 paradigm on all subjects before and after the treatment for direct comparison.

Case 1:

A 42 year old male (P1) with a history of Type 1 DM presented with the complaint of a spot in his peripheral vision in the right eye. Best corrected visual acuities (BCVA) were 20/25 OD and 20/20 OS. He was diagnosed to have moderate non-proliferative diabetic retinopathy (NPDR) in both eyes with DME in the right eye. He had no previous treatment with either anti-VEGF or laser in either eye. The subject was treated with 577-nm SML. In follow up, the subject reported reduction in the size of the blurry patch within the visual field. Clinical SD-OCT images and thickness maps before and after treatment are shown in Figure 1 (A)–(D). Post-operative BCVAs remained unchanged.

Case 2:

A 52 year old male (P2) with a history of Type 2 DM presented for diabetic examination. He had no vision complaints. Visual acuities were 20/20 OU. He was diagnosed to have moderate NPDR in both eyes with DME in the left eye. He had no previous treatment with either anti-VEGF or laser in either eye. He was treated with 577-nm SML. In follow up, his vision remained stable and the clinical SD-OCT images were also stable. Clinical SD-OCT images and thickness maps before and after treatment are shown in Figure 2 (A)–(D). Post-operative BCVAs remained unchanged.

Case 3:

A 57 year old male (P3) with Type 2 DM presented for diabetic examination. He had a history of a macula-involving rhegmatogenous retinal detachment that had been previously treated with a combined scleral buckle and pars plana vitrectomy in the left eye. He had also undergone cataract surgery with an intraocular lens implant in both eyes. Over the two years following his retinal detachment repair, he developed diabetic retinopathy. Visual acuities on presentation were 20/70- OD and 20/25+ OS. He was diagnosed to have moderate NPDR in both eyes and DME in the left eye. With the exception of the laser used in the repair of his retinal detachment, he had no previous treatment with either anti-VEGF or laser in the left eye. He was treated with 577-nm SML. In follow up, he showed improvement in vision in the left eye to 20/20 with improved clinical SD-OCT images.

Case 4:

A 51 year old male (P4) with recently diagnosed Type 2 DM presented for diabetic examination. He reported a loss of depth perception. Visual acuities were 20/70- OD and 20/60- OS. Five months prior, he received a single intravitreal dose of 1.25 mg bevacizumab and panretinal photocoagulation for proliferative diabetic retinopathy (PDR) complicated by DME. On presentation, he was noted to have quiescent PDR in both eyes and DME in the right eye. He was treated with 577-nm SML. In post-treatment follow up, his visual acuity subjectively improved, and the clinical SD-OCT images also showed improvement. His

uncorrected visual acuity remained stable in the OD, but with an updated refraction, his BCVA improved to 20/30 OD.

For the AO imaging, the tenets of the Declaration of Helsinki were observed and the protocol was approved by the Institutional Review Board of The Ohio State University (OSU). Written informed consent was obtained after all procedures were fully explained to the subjects and prior to any experimental measurements.

Clinical treatment and testing

SML treatment was provided by a 577-nm yellow diode laser system (IQ577, Iridex Corporation, Mountain View, CA). All subjects had AO imaging at 2 time points: pre-treatment and at least 2 months post-treatment, additionally P1 was imaged at 6 months post-treatment. SML treatment was performed after pupil dilation and topical anesthesia. The lens used for treatment was the Mainster Focal/Grid (Ocular Instruments, Bellevue, WA), with a magnification of 1.05. Reported parameters for SML have been variable. Based on previously reported studies¹²⁻¹³, the procedure was performed with the 577-nm yellow laser utilizing the following parameters: 200 μm spot size on slit lamp (208 μm spot size on the retina), 5% duty cycle of 0.2 seconds, 400 mW power, and number of spots varying according to the extent of the DME. A 7×7 grid of spots with zero spacing was utilized. For three of the four subjects, this grid was repeated up to five times throughout the DME area and its surround. The area of targeted treatment was determined by clinical SD-OCT image and fluorescein leakage. Only SML was utilized in this cohort. No conventional threshold treatment was delivered. Additionally, no subjects received any additional treatment including intravitreal anti-VEGF or steroid during the time period studied.

AO-OCT-SLO Imaging

The AO-OCT-SLO¹⁴ was used to image retinal locations that included the DME and its surround based on the macular thickness maps generated from the clinical SD-OCT. Briefly, two separate light sources are used for the two AO imaging modalities: 680 nm for the SLO and 860 nm for the OCT. The AO system measures ocular aberrations using a Hartmann Shack wavefront sensor and corrects for them using a 97-actuator deformable mirror (DM) (ALPAO, Montbonnot, France). Prior to imaging, pupils were dilated using 1% tropicamide and 2.5% phenylephrine. Trial lenses were placed in the system to correct for the bulk of sphere and cylinder aberration. During imaging, the subject looked at a fixation target displayed on a computer monitor, which corresponded to the desired imaging location. The target was then moved to the next retinal location and the imaging repeated in order to build the larger retinal montages. A chin and forehead rest were used to stabilize the subject's head. The AO system simultaneously acquired *en face* SLO frames and OCT B-scans at 60 Hz. The field of view of the SLO was $1^\circ \times 1.7^\circ$ (horizontal \times vertical) and the B-scan was 1.7° (vertical). Adjacent AO images were montaged together to create a larger image for each subject. Depending on the size and extent of DME, the number of retinal imaging locations varied for each subject to ensure that the DME and its surround were imaged.

Data analysis

Custom MATLAB software was used to register and average AO images to improve the signal-to-noise ratio as well as to quantify parameters of individual cone photoreceptors such as inner and outer segment lengths (ISL, OSL). Figure 3 shows example SLO and OCT images from a healthy control subject. The AO-SLO image is shown in (A) illustrating a clear and contiguous cone mosaic from 1° SR to 3.5° SR. (B) shows the simultaneously acquired AO-OCT B-scan showing clear, resolved individual cone photoreceptors.

The ISL and OSL were measured to assess the integrity of cone photoreceptors at each time point. Total retinal thickness (TRT) was also measured to monitor the resolution of the edema. This endpoint was selected in contrast to the more commonly utilized central foveal thickness (CFT) due to the fact that the patients selected for this study had non-central DME. Figure 3 (B) illustrates the measurement of each of these parameters. ISL is defined as the distance between external limiting membrane (ELM) and the IS/OS junction; OSL between IS/OS junction and the cone outer segment tip (COST); and TRT between internal limiting membrane (ILM) and Bruch's membrane (BM). Ten measurements were repeated for each parameter per image and then averaged. These parameters were measured on all the AO-OCT images classified into 3 groups, based on location with respect to the DME: (i) within the DME, (ii) in-between the DME and an unaffected area, and (iii) an unaffected area (i.e., normal retinal thickness). Results were compared for statistically significant differences before and after the treatment using multiple *t*-tests. P value less than 0.05 was considered statistically significant.

RESULTS

Figure 1 (A) shows the retinal thickness map from the clinical SD-OCT indicating the DME area (*black arrow*) for the right eye of subject, P1. Figure 1 (B) is the SD-OCT B-scan clearly showing the DME. Figure 1 (C) and (D) show the equivalent images after 2 months post-treatment. Figure 1 (E)–(G) are the AO-SLO montages pre-treatment, and at 3 and 6 months post-treatment, respectively. The AO-SLO image is approximately 3° x 4°, ranging from 2–4° temporal (T) and 4–8° inferior (I) from the fovea. The DME is located at 4° T 7° I and obscures visualization of the cones at this location in both the AO-OCT and AO-SLO, but they become clearer away from the edematous area. Hard exudates are clearly visible as highly reflective areas lying above the cone photoreceptor mosaic. After the treatment, there was re-arrangement of the hard exudates, the cone mosaic became progressively clearer with good image quality throughout the AO-SLO montage at 6 months post-treatment. Figure 1 (H) shows AO-OCT B-scans from the three retinal locations pre-treatment: (i) within the DME, (ii) in-between the DME and unaffected area, and (iii) unaffected area. The AO-OCT focus was set to be at the plane of the photoreceptors. Figure 1 (I) and (J) show the corresponding AO-OCT images at 3 and 6 months post-treatment respectively. After the SML treatment, the TRT decreased and the cones and the COST reflectance became clearer within the DME. Collectively, the clear visualization of the cone mosaic in the AO-SLO images and the ability to measure both the ISL and OSL in the AO-OCT images indicates that the cones have not been structurally affected by the SML treatment.

Figure 2 shows equivalent images from the left eye of subject, P2. (A) and (B) show the retinal thickness map from the SD-OCT and the high resolution SD-OCT scan through the DME (*black arrow*) pre-treatment, respectively. The DME is located in the horizontal temporal retina, 7°T 1.5° superior (S). (C) and (D) show the corresponding images post-treatment. Figure 2 (E) and (F) show pre- and post-treatment AO-SLO montages of the DME region. Post-treatment images for this subject were only taken at 2 months. (G) and (H) show pre- and post-treatment AO-OCT images from: (i) within the DME, (ii) in-between the DME and unaffected area, and (iii) unaffected area. For this subject, the photoreceptors were not imaged as clearly in either the AO-SLO or AO-OCT channels. However, qualitatively, the photoreceptors in both imaging modalities became more visible after the treatment.

Figure 4 shows TRT, ISL and OSL measurements from the AO-OCT images at pre-treatment and 2 months post-treatment for all 4 subjects from (i) over the edematous area and (ii) from the unaffected area. In some subjects, the visibility of the photoreceptors was obscured by the presence of the overlying DME, particularly pre-treatment, making it difficult to make reliable measurements of the ISL (2 of 4 subjects) and the OSL (3 of 4). These are marked as 'not measurable' (NM) in Figure 4 (B) and (C). In some of these cases, the OSL became visible at the DME location post-treatment; in other subjects the OSL continued to be obscured as the DME was not fully resolved. Statistically significant changes are marked with an asterisk and the error bars are plus/minus one standard deviation.

The short-wavelength SML treatment appeared more effective for subjects P1 and P2 than for P3 and P4, based on statistically significant reduction of the TRT (at most locations) with mostly insignificant changes for the other parameters. Subject P3 shows very similar TRT measurements before and after treatment across all retinal locations. Subject P4, showed a slight thickening of the retina within the DME area post-treatment. The clinical SD-OCT showed improved resolution of the edema in 3 of the 4 subjects.

For the ISL measurements shown in Figure 4 (B), the ISL became measurable post-treatment in the DME area and remained unchanged in the unaffected location for subject P1. For the remaining subjects, the ISL differences (although statistically significant at several locations) were very small, a few micrometers in most cases, and were comparable to the axial resolution of the AO-OCT system. A consistent result across all 4 subjects was no statistically significant change in OSL pre- and post-treatment in the unaffected areas (and also within the DME for subject 4) - Figure 4 (C).

Cone densities using the AO-SLO images were difficult to measure reliably pre-treatment, however measurements were able to be made away from the DME post treatment. Cone densities in the unaffected areas post treatment for all four subjects were: P1 (2°T 5°I) - 13,322 cones/mm²; P2 (5°T 1.5°S) - 13,596 cones/mm²; P3 (0.75°S) - 30,913 cones/mm²; and P4 (7°N 2°S) - 9,158 cones/mm². All values were in good agreement with histological measurements at the same retinal locations.¹⁵ These findings coupled with generally good cone visibility in the AO-SLO images suggest that the cone photoreceptors are preserved and structurally intact after the short-wavelength SML treatment. Moreover, visual acuity

improved or remained stable in all subjects and none showed evidence of damage to the retina following the SML either by conventional clinical measurements or through AO imaging.

DISCUSSION

In this study, 3 of the 4 of subjects showed OCT evidence of improved DME following treatment with SML. Advanced AO imaging following treatment demonstrated preservation of the cone structures and failed to show any laser damage in any subject. This supports previous work by Kwon et al.¹⁶ who showed a short-term efficacy of SML at the 577-nm wavelength in treating DME by demonstrating a reduction in the central macular thickness and an improvement in vision over a period of 8 months post-treatment. They reported no evidence of clinical retinal damage induced by the shorter wavelength laser application. They also pointed out that theoretically, the 577-nm wavelength provides excellent lesion visibility during application, low intraocular light scattering, less pain and negligible xanthophylls absorption. Furthermore, the 577-nm wavelength has the advantage of being better absorbed by melanin than the 810-nm wavelength laser, which makes it better suited for selective targeting of RPE cells. Our results support previous reports that SML appears to be effective in reducing the DME without causing structural damage to the underlying photoreceptor layer.

Acknowledgments:

This work was supported by Department of Defense (DoD) Telemedicine and Advanced Technology Research Center (TATRC) grant W81XWH-10-1-0738, and NIH R01 grant EY020901. Supporting sponsors had no involvement in the study design, collection, analysis or interpretation of data, writing the manuscript, or in the decision to submit the manuscript for publication. We thank William Bloom for his help in subject recruitment.

REFERENCES

- Centers for Disease Control and Prevention, <http://www.cdc.gov/diabetes/data/statistics/2014statisticsreport.html>
- Klein R, Klein BE, Moss SE, et al. The Wisconsin epidemiologic study of diabetic retinopathy. III. Prevalence and risk of diabetic retinopathy when age at diagnosis is 30 or more years. *Arch Ophthalmol* 1984; 102:527–32. [PubMed: 6367725]
- Photocoagulation for diabetic macular edema. Early Treatment Diabetic Retinopathy Study report number 1. Early Treatment Diabetic Retinopathy Study research group. *Arch Ophthalmol* 1985; 103:1796–806. [PubMed: 2866759]
- Lavinsky D, Cardillo JA, Melo LA Jr, et al. Randomized clinical trial evaluating mETDRS versus normal or high-density micropulse photocoagulation for diabetic macular edema. *Invest Ophthalmol Vis Sci* 2011; 52:4314–23. [PubMed: 21345996]
- Schatz H, Madeira D, McDonald HR, et al. Progressive enlargement of laser scars following grid laser photocoagulation for diffuse diabetic macular edema. *Arch Ophthalmol* 1991; 109:1549–1551. [PubMed: 1755735]
- Roider J Laser treatment of retinal diseases by subthreshold laser effects. *Semin Ophthalmol* 1999; 14:19–26. [PubMed: 10790572]
- Maeshima K, Utsugi-Sutoh N, Otani T, et al. Progressive enlargement of scattered photocoagulation scars in diabetic retinopathy. *Retina* 2004; 24:507–511. [PubMed: 15300070]
- Luttrull JK, Dorin G. Subthreshold diode micropulse photocoagulation as invisible retinal phototherapy for diabetic macular edema. A review. *Curr Diab Rev* 2012; 8:274–84.

9. Takatsuna Y, Yamamoto S, Nakamura et al. Long-term therapeutic efficacy of the subthreshold micropulse diode laser photocoagulation for diabetic macular edema. *Jpn J Ophthalmol* 2011; 55:365–369. [PubMed: 21647567]
10. Luttrull JK, Sinclair SH. Safety of transfoveal subthreshold diode micropulse laser for fovea-involving diabetic macular edema in eyes with good visual acuity. *Retina* 2014; 34:2010–2020. [PubMed: 24837050]
11. Vujosevic S, Martini F, Longhin E, et al. Subthreshold micropulse yellow laser vs. subthreshold micropulse infrared laser in center-involving diabetic macular edema: morphologic and functional safety. *Retina* 2015; 35(8):1594–603. [PubMed: 25719988]
12. Inagaki K, Ohkoshi K, Ohde S, et al. Comparative efficacy of pure yellow (577-nm) and 810-nm subthreshold micropulse laser photocoagulation combined with yellow (561–577-nm) direct photocoagulation for diabetic macular edema. *Jpn. J. Ophthalmol* 2015; 59(1):21–8. [PubMed: 25392274]
13. Figueira J, Khan J, Nunes S, et al. Prospective randomised controlled trial comparing sub-threshold micropulse diode laser photocoagulation and conventional green laser for clinically significant diabetic macular oedema. *Br. J Ophthalmol* 2009; 93(10):1341–1344. [PubMed: 19054831]
14. Wells-Gray EM, Choi SS, Zawadzki RJ, et al. Volumetric imaging of rod and cone photoreceptor structure with a combined adaptive optics-optical coherence tomography-scanning laser ophthalmoscope. *J. Biomedical Optics* 2018; 23(3).
15. Curcio CA, Sloan KR, Kalina RE, et al. Human photoreceptor topography. *J. Comparative Neurology* 1990; 292(4): 497–523.
16. Kwon YH, Lee DK, Kwon OW, The Short-term Efficacy of Subthreshold Micropulse Yellow (577-nm) Laser Photocoagulation for Diabetic Macular Edema. *Korean J Ophthalmol* 2014; 28(5):379–385. [PubMed: 25276079]

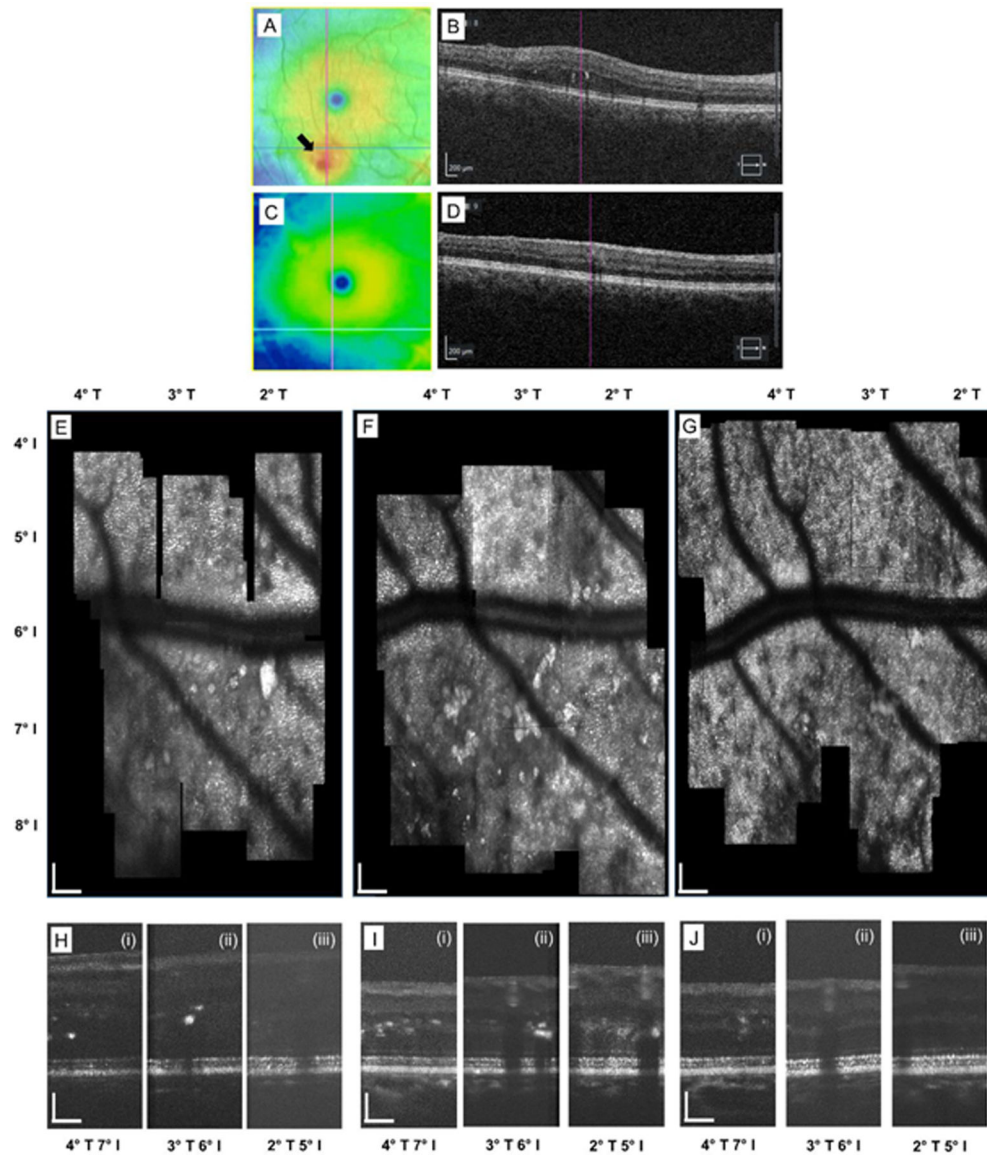


Figure 1.

Montaged AO-SLO images and AO-OCT B-scans from the right eye of P1. (A) SD-OCT retinal thickness map clearly showing the DME area (*black arrow*), and (B) is the SD-OCT B-scan pre-treatment. (C) and (D) shows the corresponding SD-OCT images post-treatment – the edema has clearly decreased. (E) shows the AO-SLO image at the pre-treatment time point, the DME is located at 4°T 7°I. (F) and (G) are the AO-SLO images at 3 and 6 months post treatment respectively. (H) AO-OCT B-scans from three retinal locations pre-treatment: (i) within the DME, (ii) in between the DME and unaffected area, and (iii) the unaffected area. (I) and (J) show the corresponding AO-OCT images at 3 and 6 months post treatment respectively. All scale bars = 100 μm.

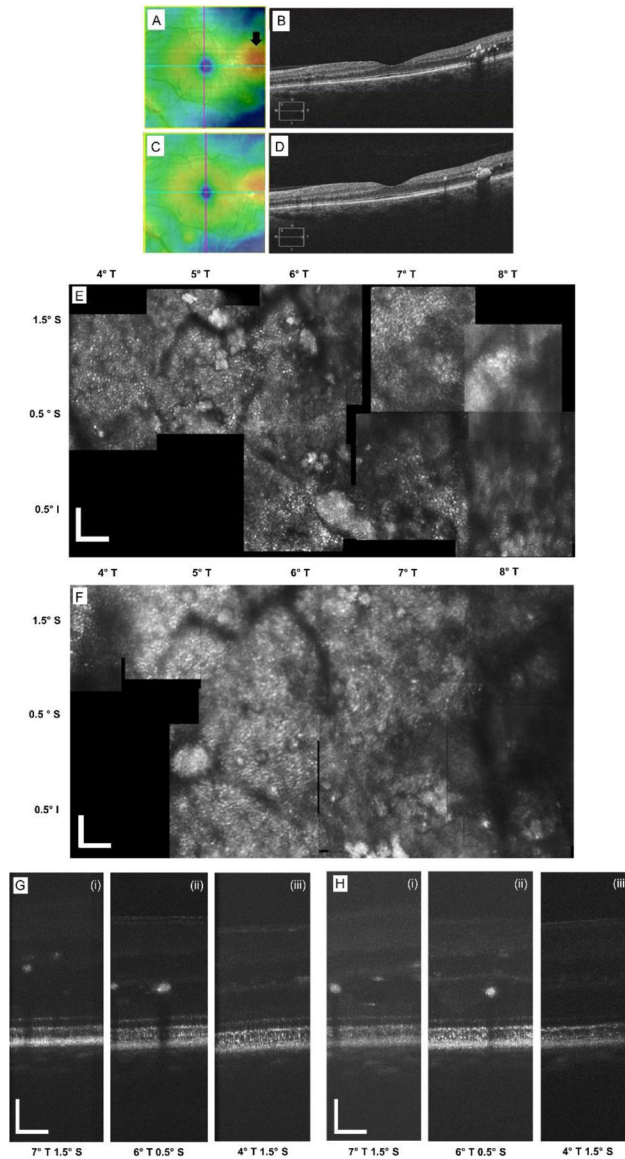


Figure 2.

Montaged AO-SLO images and AO-OCT B-scans from the left eye of P2. (A) and (B) SD-OCT retinal thickness map from the indicating the DME area (*black arrow*) and the B-scan pre-treatment. (C) and (D) shows the corresponding SD-OCT images post-treatment. (E) shows the AO-SLO image pre-treatment, the DME is located at 7°T 1.5°S. (F) AO-SLO image at 3 months post treatment. (G) AO-OCT B-scans from three retinal locations pre-treatment: (i) within the DME, (ii) in between the DME and unaffected area, and (iii) the unaffected area. (H) Corresponding AO-OCT image at 3 months post-treatment. All scale bars = 100 μ m.

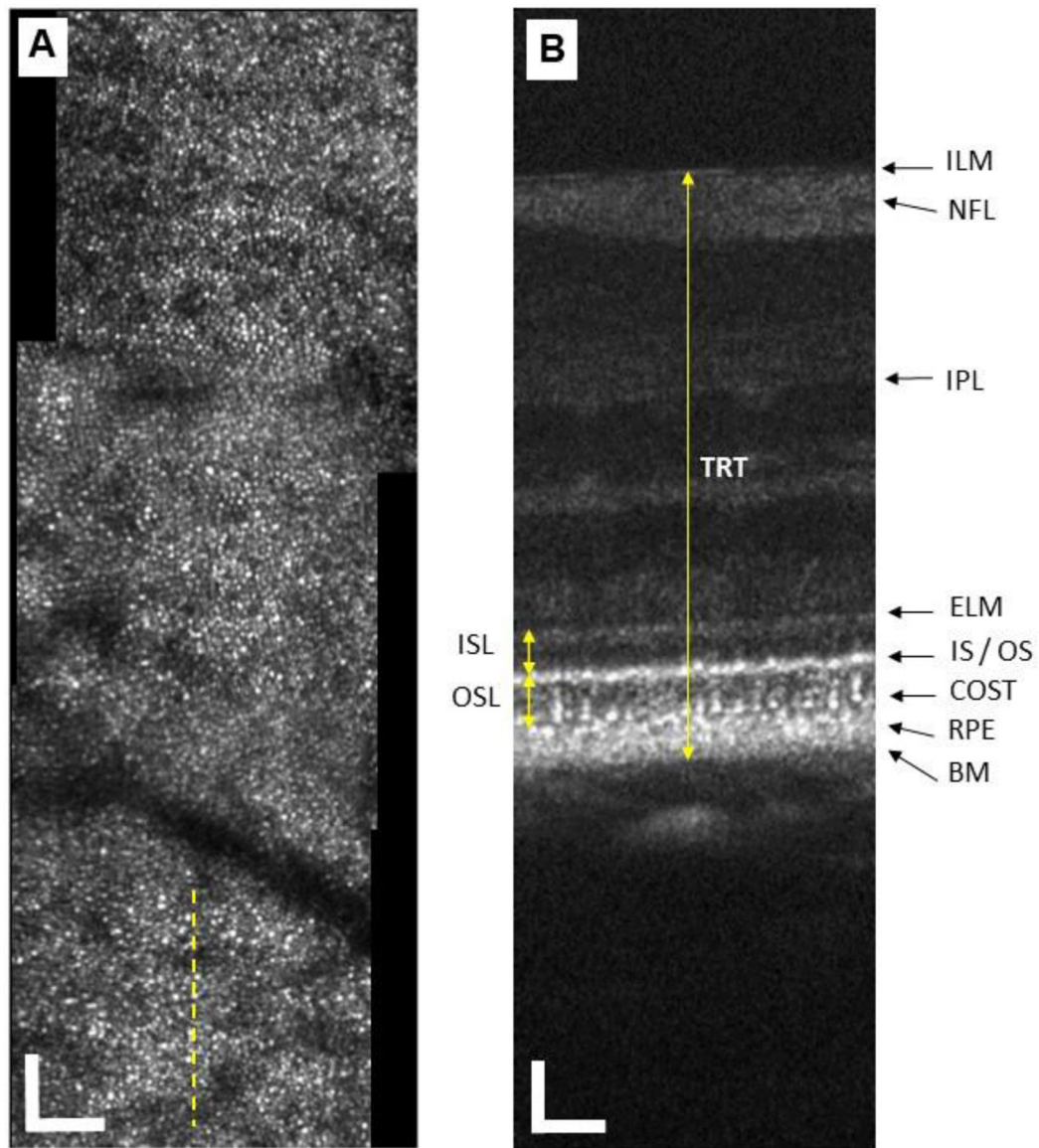


Figure 3.

(A) AO-SLO image from a healthy control subject at 1° SR to 3.5° SR, a clear mosaic of cone photoreceptors is visible throughout the image. The dashed yellow line shows the location of the simultaneous AO-OCT B-scan shown in (B). (B) AO-OCT B-scan showing a clear lateral breakup of the IS/OS junction and COST layers laterally allowing for intra-cone measurements, the various measurement parameters are also illustrated. ISL is defined as the length between ELM and IS/OS junction, OSL between IS/OS junction and cone outer segment tip (COST), and TRT between internal limiting membrane (ILM) to Bruch's membrane (BM). NFL – nerve fiber layer; IPL – inner plexiform layer; RPE – retinal pigment epithelium. All scale bars = $50\ \mu\text{m}$.

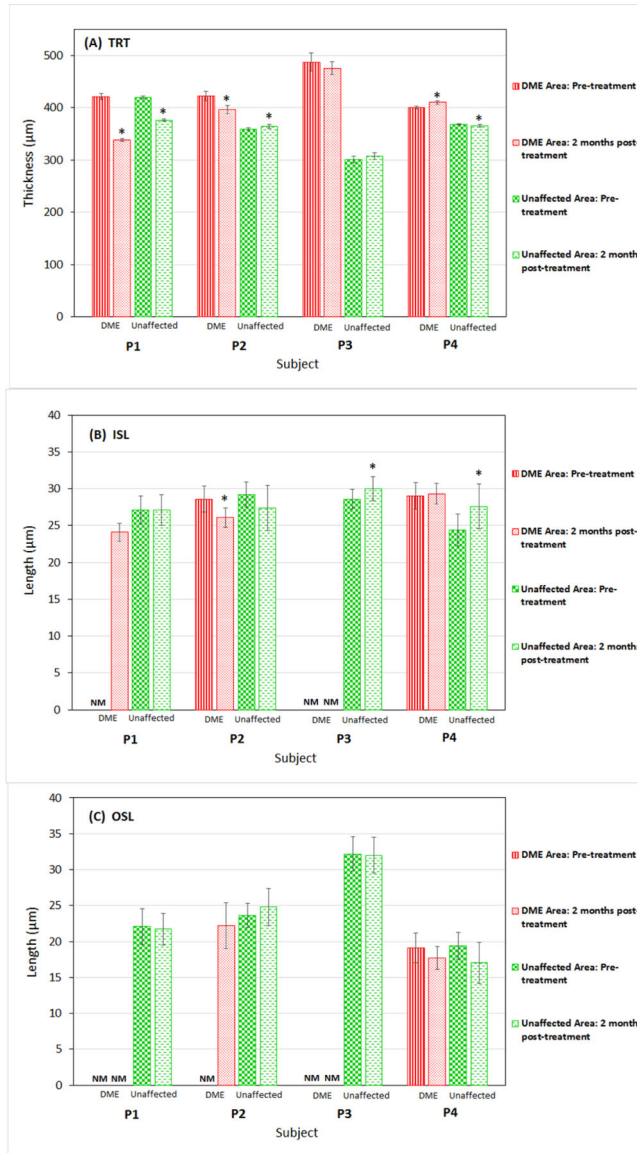


Figure 4. Retinal measurements pre- and 2 months post-treatment for all four subjects. (A) TRT measurements. Red vertical column is the TRT pre-treatment and the red dotted column the value after treatment with the DME area. Green checkered pattern and the green dashed columns show the corresponding values for the unaffected area. (B) Corresponding measurements of the ISL, same color and pattern coding as for (A). (C) OSL measurements. Statistically significant changes after treatment are marked by an asterisk. When parameters were not measurable due to the presence of the DME they have been labeled ‘NM’. Error bars are \pm one standard deviation.